

Selectivity in the Oxidative Addition of C–S Bonds of Substituted Thiophenes to the $(C_5Me_5)Rh(PMe_3)$ Fragment: A Comparison of Theory with Experiment

Tülay A. Ateşin and William D. Jones*

Department of Chemistry, University of Rochester, Rochester, New York 14627

Received May 30, 2008

Theoretical studies were performed on the C–S bond activation reactions of 2-/3-cyanothiophene, 2-/3-methoxythiophene, and 2-/3-methylthiophene with the $[Rh(PMe_3)(C_5Me_5)]$ fragment to compare with the selectivity of these reactions observed in the experimental study, with the goal of determining whether the latter represent kinetic or thermodynamic products. Density functional theory (DFT) calculations have been used to optimize the ground-state structures of the two possible insertion products and the transition state structures leading to the formation of the products arising from the above cleavage reactions to address this question. With the 2-cyano and 2-methoxy substituents, the observed formation of one product resulting from the exclusive insertion of the rhodium into the more hindered substituted C–S bond was found to be consistent with the calculated energy differences between the ground states of the two possible products (7.6 and 2.6 kcal mol⁻¹). With 2-methylthiophene, the product resulting from the activation of the unsubstituted C–S bond is calculated to be favored by 5.8 kcal mol⁻¹, in agreement with observed results. The ~1:1 ratio of products with 3-cyano and 3-methyl substituted thiophenes are also found to be consistent with the small calculated energy differences (0.4 and 0.8 kcal mol⁻¹) between the ground states of the two insertion products. Although the observed high selectivity in the formation of a single C–S bond activation product with 3-methoxythiophene appears to be underestimated in the calculations, the observed products for all substituted thiophenes correlate with the calculated thermodynamic products. In addition, the kinetic selectivities predicted based on the calculated C–S bond activation barriers are different from those observed experimentally. Consequently, these investigations demonstrate that DFT calculations can be used reliably to differentiate if an experimentally observed C–S bond activation reaction proceeds under thermodynamic or kinetic control.

Introduction

The cleavage of carbon–sulfur bonds is a necessary step in the hydrodesulfurization (HDS) process,¹ which is the process that removes sulfur from petroleum. To better understand the reaction mechanism of this heterogeneous process, the insertion of metal atoms into the C–S bonds of thiophenes is widely studied in homogeneous HDS models.² When an asymmetrically substituted thiophene is activated, two different C–S bond activation products can be formed. To probe the selectivity of this process, several thiophenes

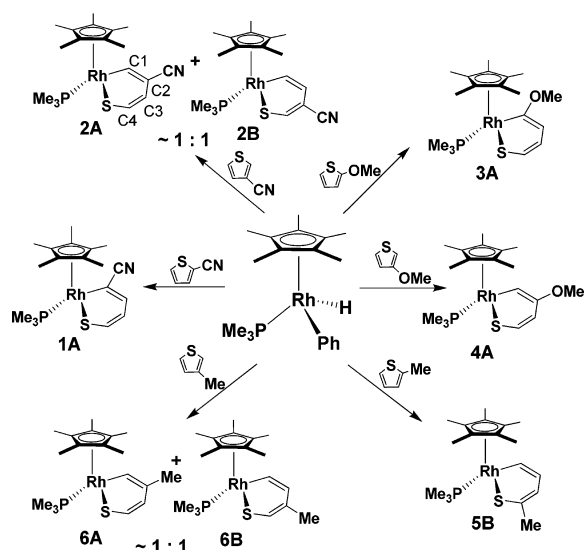
possessing a variety of substituents with differing electronic and steric effects were reacted with the reactive coordinatively unsaturated $[(C_5Me_5)Rh(PMe_3)]$ fragment, which is both an experimentally³ and a theoretically⁴ well-studied homogeneous model system (Scheme 1).

* To whom correspondence should be addressed. E-mail: jones@chem.rochester.edu.

(1) Schuman, S. C.; Shalit, H. *Catal. Rev.* **1970**, *4*, 245. (a) Topsøe, H.; Clausen, B. S. and; Massoth, F. E. *Hydrotreating Catalysis*; Springer-Verlag: Berlin, 1996.

(2) (a) Sanchez-Delgado, R. A. *J. Mol. Chem.* **1994**, *86*, 287. (b) Bianchini, C.; Meli, A. *J. Chem. Soc., Dalton Trans.* **1996**, 801. (c) Bianchini, C.; Meli, A. *Acc. Chem. Res.* **1998**, *31*, 109. (d) Bianchini, C.; Meli, A. *Transition Metal Sulphides. Chemistry and Catalysis*; Weber, T., Prins, R., van Santen, R. A., Eds; Kluwer: Dordrecht, 1998; NATO ASI Series, Vol. 60, pp 129–154. (e) Sanchez-Delgado, R. A. *Organometallic Modelling of the Hydrodesulfurization and Hydronitrogenation Reactions*; Kluwer Academic Publishers: Dordrecht, 2002.

(3) (a) Jones, W. D.; Dong, L. *J. Am. Chem. Soc.* **1991**, *113*, 559. (b) Dong, L.; Duckett, S. B.; Ohman, K. F.; Jones, W. D. *J. Am. Chem. Soc.* **1992**, *114*, 151. (c) Myers, A. W.; Dong, L.; Atesin, T. A.; Skugrud, R.; Jones, W. D. *Inorg. Chim. Acta* **2008**, *361*, 3263.

Scheme 1. Observed Reactivity of $[\text{Cp}^*\text{Rh}(\text{PMe}_3)]$ with Substituted Thiophenes

In these selectivity studies, it was found that the thermal reaction ($\sim 65^\circ\text{C}$) of $(\text{C}_5\text{Me}_5)\text{Rh}(\text{PMe}_3)(\text{Ph})\text{H}$ with 2-methylthiophene led to the exclusive formation of one product resulting from the insertion of the rhodium atom into the less hindered unsubstituted C–S bond. No evidence was observed for the formation of the other insertion product during the course of the reaction or after continued heating. On the other hand, with 3-methylthiophene, both products were observed in $\sim 1:1$ ratio.^{3a,b}

The effects of electron donating and withdrawing groups on the selectivity of C–S bond activation of thiophenes were also studied by adding the methoxy and cyano substituents onto the thiophene ring, respectively. While the thermal reaction of $(\text{C}_5\text{Me}_5)\text{Rh}(\text{PMe}_3)(\text{Ph})\text{H}$ with 2-/3-methoxythiophene and 2-cyanothiophene led to the formation of only one product resulting from insertion into the more hindered C–S bond, with 3-cyanothiophene both products were observed in a $\sim 1:1$ ratio, which did not change over time.^{3c}

In the experimental studies, single insertion products were observed with most of the thiophenes examined, but it was not clear whether these represent thermodynamic or kinetic products since only one unchanging product distribution is observed. The regioselectivities seen in these oxidative addition reactions are clearly not only influenced by sterics but also by an electronic contribution. Consequently, in this paper, density-functional theory (DFT) calculations were used to determine if the experimental results represent kinetic or thermodynamic products. The thermodynamic preference of the C–S bond activation reactions was explored by comparing the ground-state energies of the two possible isomeric products. To study the kinetic selectivities, the transition state structures for all possible bond activation reactions were optimized, and the barriers to C–S cleavage calculated with respect to the total energy of free fragments and also from

Table 1. Selected Calculated and Observed Structural Parameters of the C–S Bond Activation Products of Substituted Thiophenes by the $[(\text{C}_5\text{Me}_5)\text{Rh}(\text{PMe}_3)]$ Fragment^a and Their Energy of Formations^b

	Rh–S	Rh–C1	C1–C2	C2–C3	C3–C4	C4–S	Rh–P	α^d	ΔG^e
S1A	2.386	2.065	1.365	1.441	1.360	1.738	2.320	13.8	–32.8
1A^c	2.344	2.057	1.359	1.429	1.352	1.714	2.258	14.3	
S1B	2.378	2.021	1.354	1.446	1.365	1.767	2.308	7.1	–25.1
S2A	2.380	2.014	1.364	1.464	1.352	1.748	2.311	6.1	–26.2
S2B	2.377	2.028	1.348	1.466	1.369	1.729	2.309	6.2	–26.6
2B^c	2.321	1.965	1.362	1.470	1.320	1.740	2.252	6.1	
S3A	2.388	2.036	1.357	1.456	1.351	1.758	2.306	19.7	–26.2
S3B	2.384	2.029	1.350	1.453	1.360	1.763	2.295	9.1	–23.6
S4A	2.377	2.048	1.352	1.459	1.350	1.751	2.290	8.4	–23.7
4A^c	2.338	2.047	1.347	1.455	1.343	1.728	2.233	4.4	
S4B	2.377	2.024	1.348	1.459	1.355	1.764	2.297	6.1	–23.0
S5A	2.386	2.065	1.354	1.454	1.351	1.751	2.312	20.9	–14.6
S5B	2.380	2.026	1.350	1.454	1.357	1.766	2.297	7.6	–20.4
S6A	2.376	2.034	1.353	1.463	1.353	1.749	2.293	7.1	–19.2
S6B	2.376	2.026	1.350	1.462	1.356	1.754	2.297	6.2	–19.9

^a Interatomic distances in Å, angles in deg. Atom numbering is as shown in Scheme 1. ^b $\Delta G/\text{kcal mol}^{-1}$. ^c X-ray crystal structure data from ref. 3c. ^d Angle between the planes defined by S–Rh–C1 and C1–C2–C3–C4–S atoms. ^e Sum of electronic and thermal free energies.

their η^2 -C,S bound precursor. These studies indicate that the fragment $[\text{Cp}^*\text{Rh}(\text{PMe}_3)]$ reacts thermally with substituted thiophenes to give thermodynamic products, a conclusion that could not be made on the sole basis of the experimental studies.

Results and Discussion

Available experimental and selected optimized structural parameters for the C–S bond activation products of 2-/3-cyanothiophene, 2-/3-methoxythiophene, and 2-/3-methylthiophene are summarized in Table 1 (compounds **1**, **2**, **3**, **4**, **5**, **6**, respectively. **A** refers to C–S cleavage closest to the substituent; **B** to cleavage furthest from the substituent; an **S** prefix refers to a stable calculated structure; a **TS** prefix denotes a calculated transition state structure). The optimized structures of all 12 possible C–S bond activation products are shown in Figure 1.

There is good agreement between the theoretical and experimental structures with the largest deviation of 0.063 Å in the Rh–C1 bond length of **S2B**, which can be attributed to disorder of the thiophene ring in the X-ray crystal structure. The six-membered metallacycles are nearly planar, with a maximum puckering angle (α) of 21° between the S–Rh–C1 and S–C4–C3–C2–C1 planes in **S5A**. Steric factors due to the interaction of the α -substitution with the methyl groups of the C_5Me_5 ligand were shown to be responsible for the observed ring deformations.⁵ The C1–C2 and C3–C4 bond lengths are indicative of a C=C double bond and those of C2–C3 are indicative of a C–C single bond. These clear bond-length alternations (short–long–short) within the thiophenic rings indicate a localized diene structure.

The most important aspect of this study is summarized in Figure 2, which shows that the calculated ground-state energies (i.e., thermodynamically preferred isomers) account for the experimentally observed selectivities in the C–S bond activation reactions of substituted thiophenes with the

(4) (a) Ateşin, T. A.; Jones, W. D. *Organometallics* **2008**, *27*, 3666. Earlier published studies reported false structures for the C–S cleavage transition states: (b) Sargent, A. L.; Titus, E. P. *Organometallics* **1998**, *17*, 65. (c) Maresca, O.; Maseras, F.; Lledós, A. *New. J. Chem.* **2004**, *28*, 625.

(5) Blonski, C.; Myers, A. W.; Palmer, M.; Harris, S.; Jones, W. D. *Organometallics* **1997**, *16*, 3819.

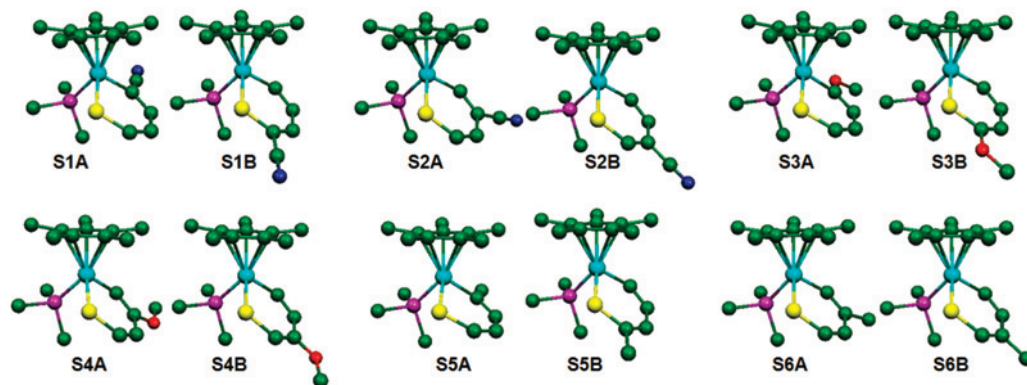


Figure 1. Optimized Structures of the C–S bond activation products of the 2-/3-methylthiophene, 2-/3-methoxythiophene, and 2-/3-cyanothiophene by the $[(C_5Me_5)Rh(PMe_3)]$ fragment.

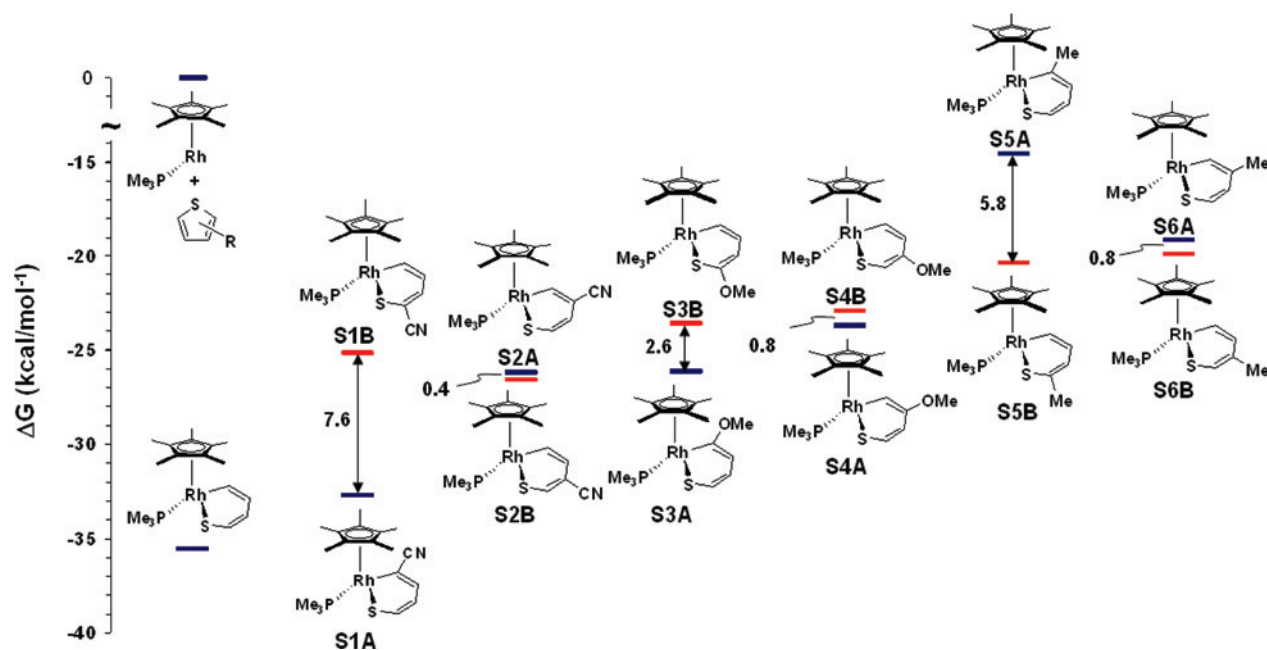


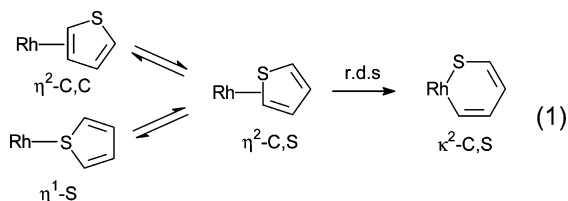
Figure 2. Calculated energetics of the C–S bond activation products of parent thiophene and substituted thiophenes by the $[(C_5Me_5)Rh(PMe_3)]$ fragment (free energies in kcal mol⁻¹ at 298 K) relative to the total energies of fragments ($[(C_5Me_5)Rh(PMe_3)]$ + thiophene/substituted thiophenes).

$[(C_5Me_5)Rh(PMe_3)]$ fragment, with only one minor exception (vide infra). The cyano and methoxy substitutions on the α -carbon of thiophene favored the formation of the insertion product resulting from the cleavage of the *substituted* C–S bond (S1A, S3A) by 7.6 and 2.6 kcal mol⁻¹, respectively, whereas the methyl substitution on the same carbon favored the cleavage of the *unsubstituted* C–S bond (S5B) by 5.8 kcal mol⁻¹. The small energy differences (0.4–0.8 kcal mol⁻¹) between the two insertion products of the substituted thiophenes at the β -carbon are consistent with the \sim 1:1 ratio of products in the reaction of 3-cyano and 3-methyl substitution thiophenes (S2A/S2B, S6A/S6B). For 3-methoxy substitution, a \sim 4:1 product ratio is calculated, but the experiment only shows the one predicted major isomeric product (S4A).

It is evident from both experimental and theoretical studies that the substitution at the 2 position of thiophene has a more significant influence on the selectivity of the C–S bond cleavage reactions compared to the substitution at the 3 position. This can be explained based on the relative thermodynamic stabilities of the two possible C–S bond

activation products. α -Cyano substituted product, 1A, would be anticipated to be more stable because of the enhanced Rh–C bond strength due to substitution at carbon with an electron withdrawing substituent. The presence of an α -methoxy carbene resonance form might contribute to the stability of 3A.^{3c}

The product mixtures seen with 3-methyl and 3-cyanothiophene are consistent with the lack of steric interactions with the C_5Me_5 or PMe_3 ligands. However, the experimentally observed high selectivity with 3-methoxythiophene exaggerates the expected 4:1 mixture of products based on the ground-state energies ($\Delta G = 0.8$ kcal mol⁻¹). This suggests that the selectivity of this reaction might be due to kinetic factors, and therefore, the transition state energies for the C–S bond activations were calculated. In our earlier theoretical studies of thiophene activation by $[(C_5Me_5)Rh(PMe_3)]$, the precursor η^2 -C,C-, η^2 -C,S-, and η^1 -S-thiophene complexes were found to be in equilibrium (eq 1), so that only the *lowest energy* transition state for C–S cleavage needed to be considered. This same approach is taken with the substituted thiophenes as outlined below.



The optimized transition state structures located for the parent thiophene activation^{4a} were used as the starting points for these C–S bond cleavage transition state calculations. There are two sets of transition states calculated for each substrate. The first set consists of isomers differing in the position of the thiophene ring, the distal carbons on thiophene being closer to either the C₅Me₅ or PMe₃ ligand (Figure 3), while the second set differs in the C–S bond being activated, substituted or unsubstituted. Hence, four transition state geometries were examined for each substrate and compared to see which was the lowest energy (i.e., leading to the kinetic product). Although there is a moderate puckering of the six-membered metallacycles toward the C₅Me₅ ligand in the C–S bond activated products, both synclinal and anticlinal transition states lead to the formation of the same ring opened product. Because the synclinal structures in which the thiophene molecule is tilted toward the C₅Me₅ ligand are lower in energy, these transition states seem to be more important than the anticlinal transition states. Therefore, the following discussions focus on these lower energy synclinal transition states.

Optimized structures for the 12 C–S bond activation transition states of 2-/3-cyanothiophene, 2-/3-methoxythiophene, and 2-/3-methylthiophene with the [(C₅Me₅)-Rh(PMe₃)] fragment are shown in Figure 4, and selected structural parameters are summarized in Table 2.⁶ There is considerable electron delocalization in the thiophenic ring between the C1, C2, C3, and C4 atoms and an average puckering angle of 61° between the S–Rh–C plane and the plane of the thiophene molecule. Also, the transition states are well advanced toward products, with Rh–S and Rh–C distances very close to the values in the final product. The C–S bond is lengthened significantly, by 0.3–0.4 Å.

Figure 5 shows the relevant transition state energies that predict the kinetic selectivities, which are *not* in agreement with the experimentally observed products. For example, the barrier to insertion into the unsubstituted C–S bond of 2-cyanothiophene (**TS1B**) is preferred by 0.6 kcal mol⁻¹ over insertion into the substituted C–S bond (**TS1A**), which would lead to the prediction that both **S1A** and **S1B** should be observed, with **S1B** being the major product. In contrast, only **S1A** is seen experimentally, which indicates that the reaction is under thermodynamic control (Figure 2). The barrier for rearrangement of **S1B** to **S1A** is calculated to be ~23 kcal/mol, and would be easily surmounted under

(6) The positive ΔG_s represent “unfavorable” species relative to the separated fragments, but calculations on other P₂Pt systems that activate substituted thiophenes show that inclusion of solvation (PCM) lowers the corresponding transition state energies by 3–6 kcal/mol. Consequently, a similar effect here would render these transition states as weakly bound transient species.

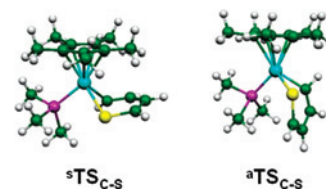


Figure 3. Optimized structures of the synclinal, ⁵TS_{C-S}, and anticlinal, ^aTS_{C-S}, C–S bond activation transition states of thiophene by the [(C₅Me₅)Rh(PMe₃)] fragment.

the reaction conditions (60 °C), thereby allowing any **S1B** that is formed to rapidly equilibrate to **S1A**. These results are also consistent with those obtained for the reaction of the [Pt(dippe)] fragment with 2-cyanothiophene, in which the kinetic isomer can actually be observed prior to its conversion to the thermodynamic isomer.⁷ Likewise, in the reaction of 3-cyanothiophene, the activation barrier for insertion into the unsubstituted C–S bond (**TS2A**) is calculated to be lower in energy by 3.1 kcal mol⁻¹ than for insertion into the substituted bond (**TS2B**), leading to the prediction that only **S2A** should be observed if the reaction is under kinetic control. When this reaction was followed experimentally by ³¹P NMR spectroscopy, no change was observed in the 1:1 ratio of the two isomeric products **S2A** and **S2B**.^{3a,b} This observation together with the calculated energies suggests that there is a fast equilibrium between the products which masks the observation of the kinetic preference for one isomer (barrier to rearrangement ~23–27 kcal/mol).

The difference in the transition state energies for insertion into C–S bonds of 2-methoxythiophene (**TS3a/TS3B**) is found to be small (0.9 kcal mol⁻¹); therefore, the observed selective formation of a single product in this reaction can also be explained in terms of the thermodynamic control indicated in Figure 2. The selectivity observed in the 3-methoxythiophene reaction for a single product indicates that calculated preference for **4A** is underestimated by at least 2 kcal mol⁻¹. The formation of **4A** is completely opposite the prediction based on the kinetic selectivity seen in Figure 5, as **TS4B** is 2.9 kcal mol⁻¹ lower than **TS4A**.

In the 2-methylthiophene reaction, the transition state energy for the substituted C–S bond activation was calculated to be 7.7 kcal mol⁻¹ higher than that for the unsubstituted C–S bond activation. In this case, the kinetic and thermodynamic selectivity predictions are the same. Although, the moderate energy difference between the bond activation barriers of 3-methylthiophene (1.4 kcal mol⁻¹) favors the cleavage of the unsubstituted C–S bond (**TS6B**), it seems that there is a fast equilibrium between the products leading to a ~1:1 ratio as in the case of 3-cyanothiophene.

Conclusions

Theoretical studies were performed on the insertion reactions of the rhodium fragment [(C₅Me₅)Rh(PMe₃)] into

(7) Ateşin, T. A.; Ateşin, A. Ç.; Skugrud, K.; Jones, W. D. *Inorg. Chem.* **2008**, *47*, 4596.

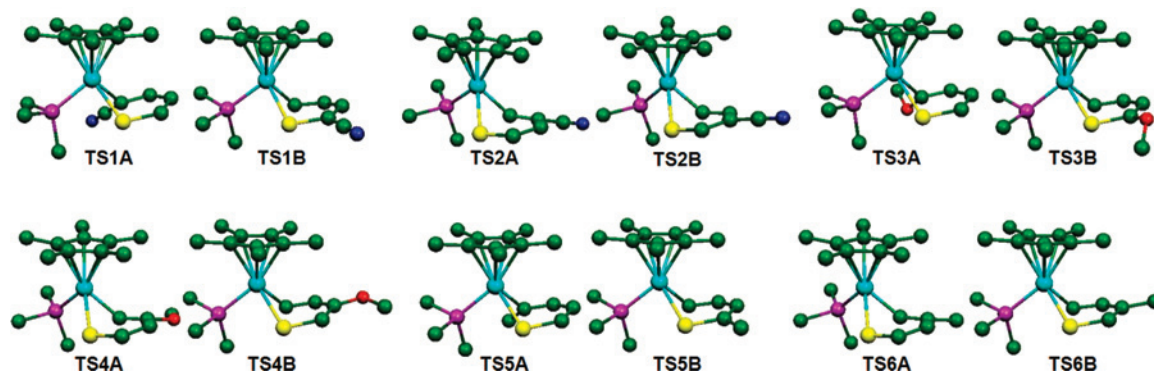


Figure 4. Optimized structures, except **TS5A**, of the C–S bond activation transition states of 2-/3-methylthiophene, 2-/3-methoxythiophene, and 2-/3-cyanothiophene by the $[(C_5Me_5)Rh(PMe_3)]$ fragment.

Table 2. Selected Structural Parameters of the C–S Bond Activation Transition States of Substituted Thiophenes by the $[(C_5Me_5)Rh(PMe_3)]$ Fragment^a and Their Energy of Formations^b from the Thiophene and the Metal Fragment

	Rh–S	Rh–C1	S–C1	C1–C2	C2–C3	C3–C4	C4–S	Rh–P	α^c	ΔG^d
TS1A	2.390	2.164	2.008	1.420	1.400	1.383	1.728	2.350	61.9	–2.2
TS1B	2.366	2.088	2.185	1.398	1.404	1.389	1.759	2.388	61.4	–2.8
TS2A	2.377	2.076	2.179	1.407	1.431	1.365	1.747	2.341	61.2	–3.3
TS2B	2.376	2.111	2.114	1.398	1.421	1.387	1.728	2.330	61.5	–0.2
TS3A	2.400	2.135	2.05	1.416	1.403	1.381	1.734	2.336	63.2	4.2
TS3B	2.388	2.126	2.100	1.394	1.414	1.379	1.769	2.315	60.5	3.3
TS4A	2.383	2.123	2.109	1.392	1.416	1.383	1.737	2.315	60.2	3.3
TS4B	2.383	2.106	2.122	1.392	1.419	1.380	1.743	2.320	61.7	0.5
TS5A	2.389	2.148	2.110	1.406	1.410	1.375	1.735	2.334	63.4	11.5
TS5B	2.386	2.114	2.123	1.392	1.417	1.376	1.752	2.319	60.4	3.8
TS6A	2.375	2.117	2.133	1.397	1.420	1.374	1.738	2.321	60.3	4.9
TS6B	2.380	2.109	2.132	1.393	1.421	1.377	1.739	2.322	60.1	3.6

^a Interatomic distances in Å, angles in deg. Atom numbering is as shown in Scheme 1. ^b $\Delta G/kcal\ mol^{-1}$. ^c Angle between the planes defined by S–Rh–C1 atoms and thiophene molecule. ^d Sum of electronic and thermal free energies.

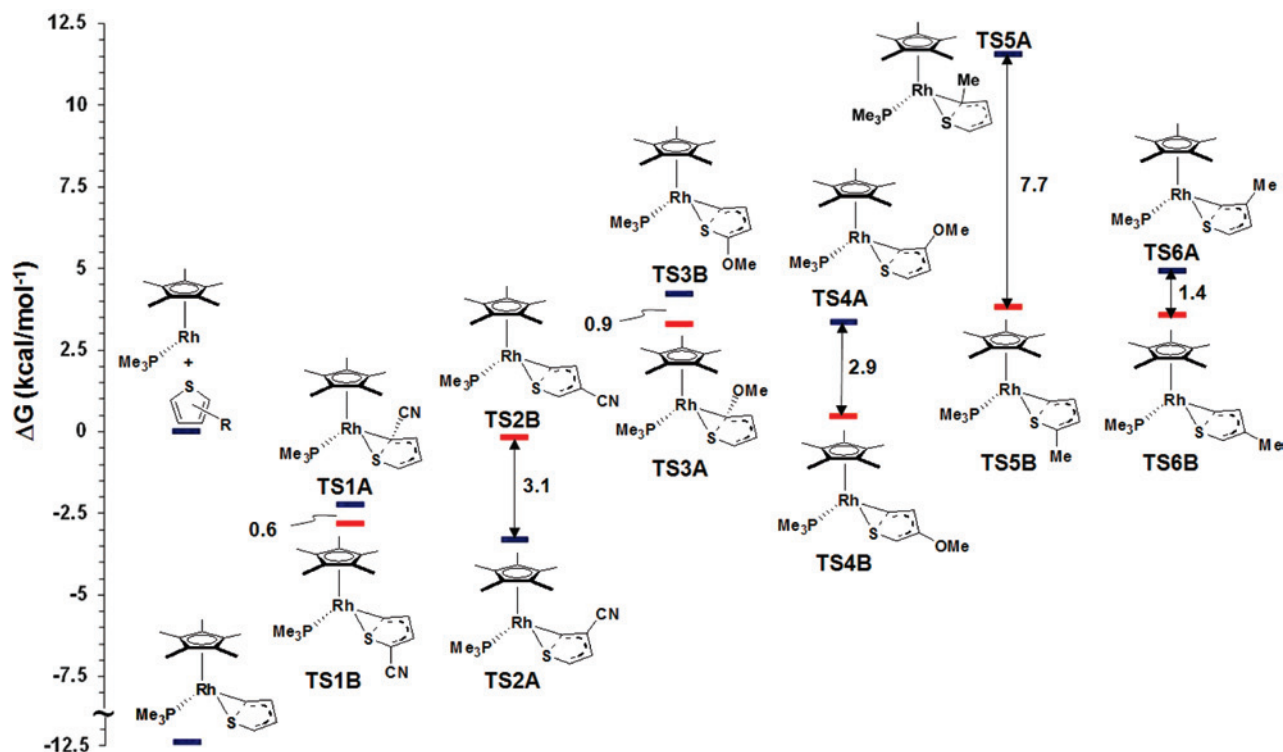


Figure 5. Energetics of the C–S bond activation transition states of parent thiophene and substituted thiophenes by the $[(C_5Me_5)Rh(PMe_3)]$ fragment (free energies in $kcal\ mol^{-1}$ at 298 K) relative to the total energies of fragments ($[(C_5Me_5)Rh(PMe_3)]$ + thiophene/substituted thiophenes).

the C–S bonds of a variety of asymmetrically substituted thiophenes to probe the selectivity of these reactions. Both optimized and, where available, X-ray crystal structures,

showed bond length alterations in the six-membered metal-lacycles and puckering angles of up to 21° between the planes defined by S–Rh–C1 and S–C4–C3–C2–C1 atoms. In

the transition state structures, the puckering angles are more pronounced with an average value of 61° , and there is extensive electron delocalization in the thiophene rings.

The high selectivity in the reactions with thiophenes substituted at the 2-positions are consistent with their relative *ground-state energies*, which favor the formation of the substituted C–S bond activation product with the 2-cyano- and 2-methoxythiophenes. These observed selectivities cannot be explained based on their calculated activation barriers. With 2-methylthiophene, the unsubstituted C–S bond activation product is formed. All observed selectivities are consistent with thermodynamic control of products. Transition states are well advanced toward the oxidative addition products.

In the reactions with 3-cyano and 3-methylthiophenes, the observed ~1:1 product ratios can also be explained based on the similar ground-state energies of the two products, not with the C–S bond activation barriers. The thermodynamic selectivity in the case of 3-methoxythiophene appears to be underestimated in the calculations but is clearly inconsistent with the kinetic product predictions. In addition, the kinetic selectivities predicted based on the calculated C–S bond activation barriers are different from those observed experimentally. Consequently, DFT methods appear to be quite useful for predicting the thermodynamic basis for selectivities in C–S bond cleavage reactions in this system, as they were in the [Pt(dippe)] system. As for kinetic selectivities, the calculated preferences are very different from the thermodynamic preferences, but the effectiveness of DFT for making kinetic predictions remains unconfirmed for the [Cp*Rh(PMe₃)] system since the initial products might not have been observed in the experiments. Kinetic selectivities were, however, accurately predicted with DFT in the [Pt(dippe)] system, leading us to believe the calculated selectivities presented here are also likely to be correct.

Experimental Section

Compounds **1–6** were prepared as described in the literature.^{3c} Selected X-ray data are included here for comparison.

Computational Methods. When available, known experimental structures for the complexes were used as the starting point for the calculations of the stable species. No simplifications were done by replacing the C₅Me₅ ligand with C₅H₅ and the PMe₃ ligand with PH₃ because of the steric and electronic contributions of methyl substituents in both C₅Me₅ and PMe₃ ligands.^{4c} The gas phase structures were fully optimized in redundant internal coordinates,⁸ with DFT and a wave function incorporating Becke's three-parameter hybrid functional (B3),⁹ along with the Lee–Yang–Parr correlation functional (LYP).¹⁰ All calculations were performed using the Gaussian 03¹¹ package. The Rh, P, and S atoms were represented with the effective core pseudopotentials of the Stuttgart group and the associated basis sets improved with a set of f-polarization functions for the transition metal ($\alpha = 1.350$, Rh),¹² and a set of d-polarization functions for the main group elements

($\alpha = 0.387$, P; $\alpha = 0.503$, S).¹³ The atoms in the thiophenic ring and the ones directly bound to the metal were represented with 6–31G(d,p)¹⁴ basis sets. As the size of the system involved in this processes still poses a challenge to current computational resources, the remaining atoms were represented with a smaller basis set (6–31G).¹⁵ The geometry optimizations were performed without any symmetry constraints. The initial guess for the transition state structures was obtained by adding the substituents onto the transition state structures located for the parent thiophene activation,^{4a} which was then optimized to a first-order saddle point. The local minima and the transition states were checked by frequency calculations. For each transition-state structure, the intrinsic reaction coordinate (IRC) routes were calculated in both directions toward the corresponding minima. The energies used throughout the text are the sum of electronic and thermal free energies calculated at 298.15 K and 1 atm. No solvent corrections were applied.

For completeness, energies of all ground states of the products and transition states leading to these products were calculated using the BLYP and BPW91 functionals. Only small effects were seen (<1 kcal/mol) in the relative energetics of the isomers (Table S1.1). The Supporting Information also includes energies of the η^2 -C,S-thiophene complexes prior to C–S cleavage.

Acknowledgment. We would like to acknowledge the NSF for financial support (CHE-0717040). We thank Simon B. Duckett, Sébastien Lachaize, and Abdurrahman Ç. Atesin for helpful discussions.

Supporting Information Available: Optimized geometries of the ground-state and transition state structures as well as the fragments in gas phase, portions of Gaussian input files for these geometry optimizations, optimized structures of the ground states, transition states, and η^2 -CS intermediates. Gibbs free energies (in kcal/mol) of the ground states, transition states, and η^2 -CS intermediates with respect to the total energy of free fragments. This material is available free of charge via the Internet at <http://pubs.acs.org>.

IC800982

(8) Peng, C.; Ayala, P. Y.; Schlegel, H. B.; Frisch, M. J. *J. Comput. Chem.* **1996**, *17*, 49.

(9) Becke, A. D. *J. Chem. Phys.* **1993**, *98*, 5648.

(10) Lee, C.; Yang, W.; Parr, R. G. *Phys. Rev. B* **1988**, *37*, 785.

- (11) Frisch, M. J.; Trucks, G. W.; Schlegel, H. B.; Scuseria, G. E.; Robb, M. A.; Cheeseman, J. R.; Montgomery, Jr., J. A.; Vreven, T.; Kudin, K. N.; Burant, J. C.; Millam, J. M.; Iyengar, S. S.; Tomasi, J.; Barone, V.; Mennucci, B.; Cossi, M.; Scalmani, G.; Rega, N.; Petersson, G. A.; Nakatsuji, H.; Hada, M.; Ehara, M.; Toyota, K.; Fukuda, R.; Hasegawa, J.; Ishida, M.; Nakajima, T.; Honda, Y.; Kitao, O.; Nakai, H.; Klene, M.; Li, X.; Knox, J. E.; Hratchian, H. P.; Cross, J. B.; Bakken, V.; Adamo, C.; Jaramillo, J.; Gomperts, R.; Stratmann, R. E.; Yazyev, O.; Austin, A. J.; Cammi, R.; Pomelli, C.; Ochterski, J. W.; Ayala, P. Y.; Morokuma, K.; Voth, G. A.; Salvador, P.; Dannenberg, J. J.; Zakrzewski, V. G.; Dapprich, S.; Daniels, A. D.; Strain, M. C.; Farkas, O.; Malick, D. K.; Rabuck, A. D.; Raghavachari, K.; Foresman, J. B.; Ortiz, J. V.; Cui, Q.; Baboul, A. G.; Clifford, S.; Cioslowski, J.; Stefanov, B. B.; Liu, G.; Liashenko, A.; Piskorz, P.; Komaromi, I.; Martin, R. L.; Fox, D. J.; Keith, T.; Al-Laham, M. A.; Peng, C. Y.; Nanayakkara, A.; Challacombe, M.; Gill, P. M. W.; Johnson, B.; Chen, W.; Wong, M. W.; Gonzalez, C.; and Pople, J. A. *Gaussian 03*; Gaussian, Inc.: Wallingford, CT, 2004.
- (12) Ehlers, A. W.; Böhme, M.; Dapprich, S.; Gobbi, A.; Höllwarth, A.; Jonas, V.; Köhler, K. F.; Stegmann, R.; Veldkamp, A.; Frenking, G. *Chem. Phys. Lett.* **1993**, *208*, 111.
- (13) Höllwarth, A.; Böhme, M.; Dapprich, S.; Ehlers, A. W.; Gobbi, A.; Jonas, V.; Köhler, K. F.; Stegmann, R.; Veldkamp, A.; Frenking, G. *Chem. Phys. Lett.* **1993**, *208*, 237.
- (14) Hehre, W. J.; Ditchfield, R.; Pople, J. A. *J. Chem. Phys.* **1972**, *56*, 2257.
- (15) Rassolov, V. A.; Ratner, M. A.; Pople, J. A.; Redfern, P. C.; Curtiss, L. A. *J. Comput. Chem.* **2001**, *22*, 976.